IN-DUCT PRESSURE MEASUREMENTS FOR SOUND POWER DETERMINATION IN FLOW-DUCTS

P F Joseph and C L. Morfey

Institute of Sound and Vibration Research, University of Southampton

1. INTRODUCTION

Exhaust mufflers, large exhaust stacks, and turbofan engines are common examples of ducted noise. The most useful measure of the sound produced by these noise sources is the sound power transmitted along the duct. Unlike acoustic pressure, sound power is a conserved quantity that provides a single index of the source strength. Its measurement, however, is difficult and must usually be inferred from a number of acoustic pressure measurements made, either inside the duct, or in the radiated far-field. A fundamental difficulty with making power measurements from in-duct pressure measurements is the presence of airflow. Munroe and Ingard [1.1] show that the usual approach of deducing acoustic particle velocity from the pressure gradient is no longer valid when the direction of flow and sound propagation differs. Under these conditions, they show that the relationship between these quantities is non-unique.

Another approach, and the one explored in this paper, is to predict the relationship between the sound power and pressure based upon an assumed mode amplitude distribution. This paper investigates the relationship between pressure and power for a number of idealized source distributions. Of particular interest here is the sensitivity of this relationship to the assumed source distribution and, in particular, the effect of flow speed. For simplicity, the analysis will be restricted to hard walled infinite ducts. It excludes (i), reflections from the open end (ii), the effects on the propagation by the shear profile, including the duct wall boundary layer, (iii), cutoff modes, (iv) measurement noise, for example, due to turbulence. The effect of these factors on sound power measurement in flow-ducts is discussed extensively in a recent paper by Neisse and Arnold [1.2].

2. MODAL SOUND TRANSMISSION

The infinite duct, and its associated co-ordinate system, is presented in Fig 1 below.

Error! Not a valid link.

Figure 1. Semi-infinite, hard walled unflanged circular duct with associated co-ordinate system and continuous source distribution represented by the shaded region.

The in-duct sound field satisfies the homogeneous wave equation given by

$$\left(\frac{1}{c^2}\frac{\overline{D}^2}{Dt^2} - \nabla^2\right)p = 0 \qquad (1)$$

where

$\frac{\overline{D}}{Dt} = \frac{\partial}{\partial t} + c\,M_x \frac{\partial}{\partial x}$ is the convected derivative operator associated with the mean flow velocity $(cM_x, 0, 0)$ in the $(x, \mathbf{y})$ system and c is the sound speed in the quiescent medium. The in-duct sound field can be expressed as the sum of modal components $p = \sum_{m=-\infty}^{\infty} \sum_{n=0}^{\infty} p_{mn}$, where (m,n) are the usual circumferential and radial mode indices. Above its cutoff frequency, at a single frequency ω, a single incident mode of amplitude a_{mn} is described by

$$p_{mn}(x, \mathbf{y}) = e^{-i\omega t} a_{mn} \Psi_{mn}(\mathbf{y}) e^{ik_{xmn} x} \tag{2}$$

Equation (2) in Eq. (1) gives

$$k_{xmn} = \left(\frac{\alpha_{mn} - M_x}{1 - M_x^2} \right) \frac{\omega}{c}, \quad \alpha_{mn} = \sqrt{1 - (\kappa_{mn}/k)^2 (1 - M_x^2)}. \tag{3a,b}$$

where κ_{mn} are a set of eigenvalues that are characteristic of the duct cross section such that the corresponding mode shape functions Ψ_{mn}, defined by $(\nabla_\perp^2 + \kappa_{mn}^2)\Psi_{mn}(\mathbf{y}) = 0$, also satisfy the duct wall boundary conditions. The sign convention adopted here is such that $M_x > 0$ represents sound propagation in the direction of the flow (duct exhaust) while $M_x < 0$ represents propagating waves in the opposite direction to the flow (duct inlet). The parameter α, which we shall call the cut-on ratio, takes values between $\alpha = 0$ precisely at the modal cutoff frequency $\omega = \omega_{mn} = \kappa_{mn} c_0 (1 - M_x^2)^{-\frac{1}{2}}$, and tends to $\alpha = 1$ as $\omega / \omega_{mn} \to \infty$, corresponding to modes well above cuton.

3. RATIO OF SOUND POWER TO MEAN SQUARE PRESSURE AVERAGE OVER A DUCT CROSS SECTION

In this paper we are concerned with the behaviour of the non-dimensional quantity β_S, defined by Eq. (4) below, from which the total transmitted sound power $\overline{W}$ may be deduced from measurements of the mean squared pressure averaged over a duct cross section, $\langle \overline{p^2} \rangle_S = \frac{1}{2} S^{-1} \int_S p p^* dS$,

$$\overline{W} = \beta_S \frac{S \langle \overline{p^2} \rangle_S}{\rho_0 c} \tag{4}$$

where ρ_0 is the mean density. We shall adopt the generalized definition of sound power flow in a uniform axial mean flow [2.1] given by

$$\overline{W} = \frac{1}{2} \int_S \left[\rho_0 c M_x u_x u_x^* + M_x p p^* / \rho_0 c + (1 + M_x^2) p u_x^* \right] dS \tag{5}$$

where u_x denotes axial particle velocity. The time averaged (mean) squared pressure at a position $(\mathbf{y}, x)$ in the duct in a narrow frequency band may written as

$$\overline{p^2}(\mathbf{y},x)=\tfrac{1}{2}E\left\{\left|\sum_{m,n}a_{mn}\Psi_{mn}(\mathbf{y})\,e^{ik_{xmn}x}\right|^2\right\} \tag{6}$$

where $E\{\}$ denotes the expectation. For incoherent excitation we treat the mode amplitudes as uncorrelated random variables so that $E\{a_{mn}a^*_{m'n'}\}=0$ for $[m,n]\neq[m',n']$, which in Eq. (6) leads to

$$\overline{p^2}(\mathbf{y})=\tfrac{1}{2}\sum_{m,n}E\left\{\left|a_{mn}\right|^2\right\}\Psi^2_{mn}(\mathbf{y}) \tag{7}$$

This situation is appropriate to many random broadband excitation mechanisms such as unsteady combustion and the turbulence-airfoil interaction responsible for broadband noise generation by fans. Averaging Eq. (6) in this way removes the dependence on x, suggesting that the mean squared pressure in the duct is axi-symmetric and also independent of the distance x along the duct. Note that the presence of reflections at the open end (which are neglected in this investigation) will introduce some axial pressure variation.

The mean squared pressure is now averaged over a duct cross-section S. Making use of the normalization property $S^{-1}\int_S \Psi^2_{mn}(\mathbf{y})dS=1$, Eq. (7) becomes

$$\left\langle\overline{p^2}\right\rangle_S=\frac{1}{S}\int_S\overline{p^2}(\mathbf{y},x)dS=\tfrac{1}{2}\sum_{m,n}E\left\{\left|a_{mn}\right|^2\right\} \tag{8}$$

This result could have been derived using the orthogonality property of the mode shape functions. Equation (8) is therefore completely general and is valid even for correlated mode amplitudes.

The modal solution of Eqs (2) and (3), together with the axial particle velocity obtained from the linearised momentum equation, substituted in (5), leads to following generalized definition of the time-averaged acoustic sound power carried by a single mode above cutoff in an axial uniform mean flow [2.1]

$$\overline{W}=\sum_{m,n}\overline{W}_{mn},\qquad \overline{W}_{mn}=\frac{S\left|a_{mn}\right|^2\alpha_{mn}}{2\rho c}\frac{\left(1-M_x^2\right)^2}{\left(1-\alpha_{mn}M_x\right)^2}, \tag{9}$$

where S is the duct cross-sectional area and the expectation has been dropped for brevity. Comparison between Eqs. (3*a*) and (11) makes explicit that the signs of α relate to the direction of energy transmission and not the direction of phase velocities. Equations (8) and (11) in (4) give the following general expression for β_S as

$$\beta_S=\left(1-M_x^2\right)^2\frac{\sum_{m,n}\dfrac{\left|a_{mn}\right|^2\alpha_{mn}}{\left(1-\alpha_{mn}M_x\right)^2}}{\sum_{m,n}\left|a_{mn}\right|^2} \tag{10}$$

4. SOURCE MODELS

4.1. UNCORRELATED SOURCES OF ARBITRARY SPATIAL AND TEMPORAL ORDER UNIFORMLY DISTRIBUTED OVER A DUCT CROSS-SECTION

In this section we derive the relationship between the mode amplitudes excited in an infinite hard walled duct containing an axial mean flow and the cut-on ratio α for incoherent sources of arbitrary spatial and temporal order, uniformly distributed over a duct cross-section. The inhomogeneous wave equation for sound in a uniform flow is

$$\left(\frac{1}{c^2}\frac{\overline{D}^2}{Dt^2} - \nabla^2\right)p = q \tag{11}$$

Common forms of q are:

$$q = \rho_0 \Gamma \qquad (\Gamma = \text{volume acceleration source distribution})$$

$$q = \rho_0 \frac{\overline{D}Q}{Dt} \qquad (Q = \text{volume velocity})$$

$$q = \rho_0 \frac{\overline{D}^2\sigma}{Dt^2} \qquad (\sigma = \text{volume displacement})$$

$$q = \nabla.\mathbf{F} \qquad (\mathbf{F} = \text{applied force distribution}) \tag{12}$$

A generalization of these possibilities is

$$q = \left(\frac{\overline{D}}{Dt}\right)^{\nu} \frac{(-\partial)^{\mu}}{\partial x_i \partial x_j \ldots} q_{ij\ldots} \tag{13}$$

which represents a source distribution of temporal order ν and spatial order μ. In what follows the source distribution is limited to axial components of q_{ij}. In this case

$$q = \left(\frac{\overline{D}}{Dt}\right)^{\nu}\left(\frac{-\partial}{\partial x}\right)^{\mu} q_{xx\ldots} \tag{14}$$

Consider a single mode excited in a semi-infinite duct by a source distribution confined to a single axial location. Under these circumstances Morfey [2.1] shows that for a single mode the spatial differentials in Eq. (13) are equivalent to

$$\left(-\frac{\partial}{\partial x}\right)^{\mu} \rightarrow (-ik_{xmn})^{\mu} \tag{15}$$

Similarly, the temporal differential in Eq. (13) may be replaced by

$$\left(\frac{\overline{D}}{Dt}\right)^{\nu} \rightarrow \left[-i\omega + U\frac{\partial}{\partial x}\right]^{\nu} = \left[-i\omega\left(\frac{1-\alpha M_x}{1-M_x^2}\right)\right]^{\nu} \tag{16}$$

Combining Eqs. (13) – (16) and following the approach described in, for example, Ref [4.1] leads to the following general expression for the mode amplitude $\left|a_{mn}^{(\mu,\nu)}\right|^2$ excited in a semi-infinite duct by an incoherent source distribution of spatial order μ and temporal order ν, uniformly distributed over a duct cross section,

$$\left|a_{mn}^{(\mu,\nu)}\right|^2 \propto \frac{1}{\alpha_{mn}^2}\left(\frac{M_x - \alpha_{mn}}{1-M_x^2}\right)^{2\mu}\left(\frac{1-\alpha_{mn}M_x}{1-M_x^2}\right)^{2\nu} \tag{17}$$

Under this indexing convention the source distributions of Eq. (17) take the index pairs: $(\mu,\nu)=(0,0)$ for volume acceleration sources, $(\mu,\nu)=(0,1)$ for volume velocity (monopole) sources, $(\mu,\nu)=(0,2)$ for volume displacement sources, and $(\mu,\nu)=(1,0)$ for axial dipole sources. For sources of non-zero spatial order, $\mu > 0$, the mode amplitudes are non-monotonic functions of the cut-on ratio α, dropping to zero at $\alpha_{mn}=M_x$. This condition occurs at the zero-Mach number cutoff frequency $\omega = c\kappa_{mn}$. Equation (17) in (10) gives the following expression for the non-dimensional ratio of incident sound power and mean square pressure averaged over a duct cross section,

$$\beta_S^{(\mu,\nu)} = \frac{\left(1-M_x^2\right)^2 \sum_{m,n} \alpha_{mn}^{-1}\left(1-\alpha_{mn}M_x\right)^{2(\nu-1)}\left(M_x-\alpha_{mn}\right)^{2\mu}}{\sum_{m,n} \alpha_{mn}^{-2}\left(1-\alpha_{mn}M_x\right)^{2\nu}\left(M_x-\alpha_{mn}\right)^{2\mu}} \tag{18}$$

4.2. EQUAL ENERGY PER MODE, AND EQUAL ENERGY DENSITY PER MODE

Two alternative source models are the assumption that all cut-on modes carry equal power, and that all cut-on modes produce equal energy density (total acoustic energy per unit volume). Evidence to support the latter as being the most appropriate model for fan noise in ventilation ducts is presented in Ref [4.2]. For 'equal energy per mode' we set in Eq. (9) $\overline{W}_{mn} = \varpi$. The resulting mode amplitude distribution $\left|a_{mn}^{(ee)}\right|^2$ is,

$$\left|a_{mn}^{(ee)}\right|^2 = 2\rho_0 c_0 S^{-1}\alpha_{mn}^{-1}\varpi\frac{\left(1-\alpha_{mn}M_x\right)^2}{\left(1-M_x^2\right)^2} \tag{19}$$

For the 'equal energy density per mode' source model we note the following generalized definition of the volume-averaged energy density $\Pi_{mn} = W_{mn}/Sc_{gmn}$, where c_{gmn} denotes the modal axial group velocity defined by ${}^{c}g_{mn} = \partial\omega/\partial k_x$. Performing the differentiation on Eq. (3*a*) yields ${}^{c}g_{mn}/c = \left(1-M_x^2\right)\alpha_{mn}/\left(1-\alpha_{mn}M_x\right)$. The resulting expression for Π_{mn} is given in Eq. (20*a*), and the mode amplitude distribution $\left|a_{mn}^{(eed)}\right|^2$ obtained by setting $\Pi_{mn} = \Pi$ is given by Eq. (20*b*),

$$\Pi_{mn} = \frac{|a_{mn}|^2}{2\rho c^2} \frac{(1 - M_x^2)}{1 - \alpha_{mn} M_x}, \qquad |a_{mn}^{(eed)}|^2 = \frac{2\Pi \rho c^2 (1 - \alpha_{mn} M_x)}{(1 - M_x^2)} \qquad (20a,b)$$

Comparison of Eqs. (19) and (20*b*) with (18) shows that, in general, the source models based on assumptions about constancy of modal energy are not members of the general family of multi-pole source distributions of Eq. (18) parameterised on (μ,ν). The single exception occurs for $M_x = 0$. At zero flow speed the 'equal energy per mode' model, the 'equal energy density per mode' model, and both the incoherent uniform distribution of monopoles and axial dipole models all collapse to the single source family, $|a_{mn}|^2 \propto \alpha_{mn}^{-2(\mu-1)}$. As discussed in Ref [4.1], values of the index μ = 3/2 and μ = 2 correspond, respectively, to equal energy per mode and a uniform distribution of incoherent monopoles. Setting μ = 1 corresponds, simultaneously, to a uniform distribution of incoherent axial dipoles and equal energy density per mode. This is because, even though the modal sound power is proportional to α, and therefore tends to zero as cutoff is approached, the speed with which this diminishing energy is transmitted along the duct, also lessens at precisely the same rate, equal to the zero-flow group velocity α. Thus in the absence of flow, an axial dipole distribution is equivalent to the assumption of constant modal energy density.

Equations (19) and (20*b*) in Eq. (10) give the following expressions for β_S for the case of equal energy per mode and equal energy density per mode

$$\beta_S^{(ee)} = N\left[\sum_{m,n} \frac{(1 - \alpha_{mn} M_x)^2}{\alpha_{mn}}\right]^{-1}, \qquad \beta_S^{(eed)} = \frac{(1 - M_x^2)^2 \sum_{m,n} \alpha_{mn} (1 - \alpha_{mn} M_x)^{-1}}{\sum_{m,n} (1 - \alpha_{mn} M_x)} \qquad (21,22)$$

where $N = N(ka,M_x)$ is the total number of propagating modes. Equations (18) – (22) are likely to be inaccurate at the low frequencies of ka < 0.5 where the presence of reflections from the open end can no longer be neglected. The present analysis will be restricted to frequencies above this.

5. COMPUTED B_S VERSUS FREQUENCY

The eigenvalues for a hard walled cylindrical duct of radius a are given by

$$\kappa_{mn} = j'_{mn} / a, \qquad (23)$$

Here, j'_{mn} is the n^{th} stationary value of the Bessel function of order *m*. Equations (18), (21) and (22) were used to compute β_S as a function of non-dimensional frequency ka between 1 and 250 in a circular duct. Predictions were obtained for the axial dipole source distribution, the monopole source distribution, and the assumption of equal energy per mode and equal energy density per mode. The results for the representative Mach numbers of $M_x = 0$, $M_x = \pm 0.1$ and $M_x = \pm 0.3$ are plotted in Figs 2 - 5. The predictions are normalized on the plane wave result, $\beta_S = (1 + M_x)^2$.

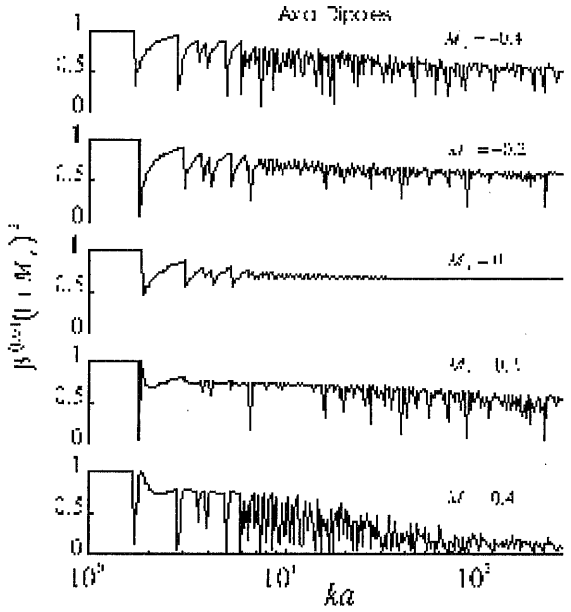

Figure 2. The ratio β_S of transmitted sound power to mean squared pressure averaged over a duct cross-section evaluated for incoherent axial dipole sources uniformly distributed over a duct cross-section for different axial Mach numbers.

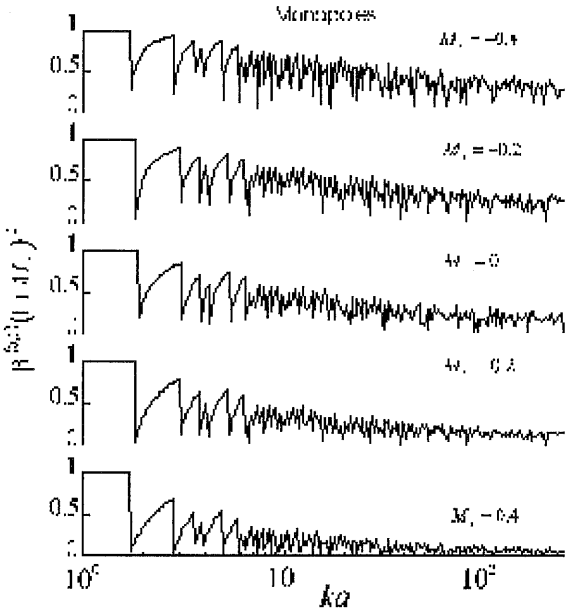

Figure 3. The ratio β_S of transmitted sound power to mean squared pressure averaged over a duct cross-section evaluated for incoherent Monopole sources uniformly distributed over a duct cross-section for different axial Mach numbers.

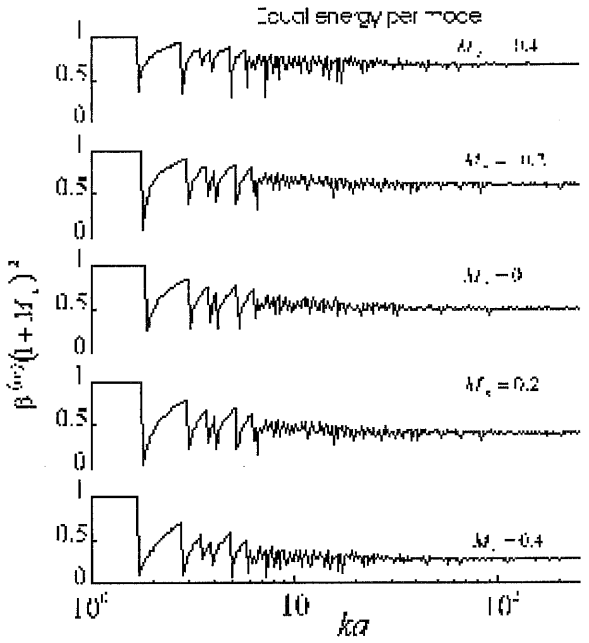

Figure 4. The ratio β_S of transmitted sound power to mean squared pressure averaged over a duct cross-section evaluated under the assumption of 'equal energy per mode' for different axial Mach numbers.

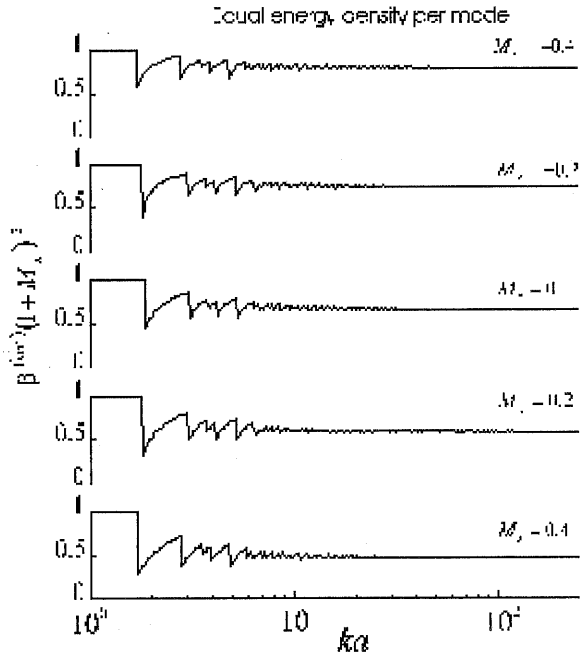

Figure 5. The ratio β_S of transmitted sound power to mean squared pressure averaged over a duct cross-section evaluated under the assumption of 'equal energy density per mode' for different axial Mach numbers.

These results suggest that the frequency variability of β_S for some source distributions are more greatly affected by flow-speed than others. The β_S-frequency-variability is observed to increase with increasing flow speed in an exhaust duct but diminish with increasing flow speed in a duct inlet. The axial dipole distribution is most sensitive to flow-speed, as clearly shown in Fig 2. At zero flow speed β_S remains within a narrow range of values over the entire frequency range. Upon the introduction of the small flow speed of $M_x = \pm 0.1$, β_S drops close to zero at the cutoff frequencies. The severity of this 'drop out' phenomenon worsens considerably with increasing M_X. For $M_x = \pm 0.3$, typical of the flow speeds in turbofan engine inlets and exhausts, fluctuations in β_S are so rapid, particularly at high frequencies where the modal density is very high, its practical application to determine sound power from acoustic pressure measurements is susceptible to large error. This cause of this behaviour is readily explained by the sensitivity of the mode amplitudes to small values of M_x at frequencies very close to cutoff. For $M_x << 1$ and $\alpha << 1$ in Eq. (18),

$$\frac{\left|a_{mn}^{(\mu,\nu)}(M_x)\right|^2}{\left|a_{mn}^{(\mu,\nu)}(0)\right|^2} \approx (1 - M_x/\alpha_{mn})^{2\mu}, \qquad (M_x << 1, \quad \alpha_{mn} << 1) \tag{24}$$

indicating that for $\mu > 0$ the mode amplitudes at cutoff are finite only for M_x precisely equal to zero. For non-zero Mach numbers the amplitudes of modes close to cutoff tend to infinity leading to the large fluctuations in β_S observed in Fig 2 for $\mu = 1$. For $\mu = 0$, however, Eq. (24) predicts that the behavior of the mode amplitudes close to cutoff are not affected by flow speed. This is verified in Fig 3 where fluctuations in β_S are not strongly influenced by M_x. The simulation results of Figs 2 – 6 may be summarized as:

- The relationship between sound power flow and the mean square pressure in a hard walled, infinite duct generally appears as a highly irregular function of frequency. Frequency irregularity arises from the behaviour of individual modes at frequencies close to their cutoff frequencies.

- The frequency irregularity of β_S for sources of non-zero spatial-order (e.g. dipoles) is more greatly affected by flow speed than sources of finite temporal order (e.g., monopole sources). This is due to the sensitivity to flow of the mode amplitudes close to cutoff

- Frequency irregularity is appreciably less for source models based on constancy of modal energy rather sources of prescribed multi-pole order

- Frequency variability increases with increasing axial Mach number in the duct exhaust, but lessens with increasing Mach number in the duct intake

- A well-defined high-*ka* asymptote only exists in some cases. We will show in Sec. VI that these are for the source distributions of equal energy per mode, equal energy density per mode at all flow speeds, and for the axial dipole distribution at zero flow speed.

6. HIGH-*ka* LIMITING BEHAVIOUR

At suitably high *ka,* the discrete summation of modes in Eq. (10) may be approximated by the integration over a continuum of modes,

$$\beta_S = \left(1 - M_x^2\right)^2 \frac{\int_0^1 \frac{|a(\alpha)|^2 \alpha n(\alpha) d\alpha}{(1 - \alpha M_x)^2}}{\int_0^1 |a(\alpha)|^2 n(\alpha) d\alpha} \qquad (ka \to \infty) \tag{25}$$

Here $n(\alpha)$ is the normalized modal density function defined by

$$n(\alpha) = \frac{N(\alpha + \delta\alpha) - N(\alpha)}{N\delta\alpha}\bigg|_{\lim \delta\alpha \to 0}, \quad \int_0^1 n(\alpha) d\alpha = 1 \tag{26}$$

where $N(\alpha)$ is the number of modes with 'α' values of between 0 and α. The high-*ka* asymptotic density function n, expressed in terms of α, is given by $n(\alpha) = 2\alpha$ [4.1]. This result in Eq. (25) evaluated for the mode amplitude distribution functions of Eqs. (19) and (20*b*) give

$$\beta_S^{(ee)} = \tfrac{1}{2}\left(1 - M_x + \tfrac{1}{3}M_x^2\right)^{-1}, \quad \beta_S^{(eed)} = \frac{6\left[1 - M_x^2\right]\left[\frac{1}{2}M_x^{-1} + M_x^{-2} + M_x^{-3}\ln(1 - M_x)\right]}{2M_x - 3}, \quad (ka \to \infty) \tag{27}$$

Evaluating Eqs. (27) for $M_x = 0$ gives

$$\beta^{(ee)} = \tfrac{1}{2}, \qquad \beta^{(eed)} = \tfrac{2}{3}, \qquad (M_x = 0, \quad ka \to \infty) \tag{28a,b}$$

Equation (28*a*) indicates that, for zero flow, the equal power per mode assumption is equivalent to a hemi-diffuse field in which acoustic energy arrives at the open end from all solid angles equally. Equation (28*b*) is identical to that predicted for the axial dipole distribution in zero-flow (Fig 2) but differs when a flow is introduced. As discussed previously, the axial dipole and equal energy density per mode model are equivalent source models at zero flow-speed.

The corresponding high-*ka* expression of Eq. (18) for the multipole source distributions, however, generally fails to converge for most (μ,ν) combinations. Whilst the numerator of Eq. (18) always converges, and hence the multi-mode transmitted sound power remains theoretically finite, the denominator, which is proportional to mean square pressure, does not. This function diverges slowly to infinity as

$$\lim_{\varepsilon \to 0} \int_\varepsilon^1 2\alpha^{-1}(1 - \alpha M_x)^{2\nu}(M_x - \alpha)^{2\mu} d\alpha \to -2M_x^{2\mu} \lim_{\varepsilon \to 0}\left[\ln \varepsilon\right] \tag{29}$$

Equation (29) explains the tendency observed in Figs 2 and 3, for β_S to approach zero with increasing *ka*, to the behaviour of modes close to cutoff. The slow logarithmic divergence of this integral indicates that any dissipation present in the duct, for which near-cutoff modes are most affected, will ensure its convergence. The range of parameters in Eq. (30) for which convergence is obtained are $\mu > 0$ and $M_x = 0$, for any value of ν. Allowing the Mach number to go to zero offsets the logarithmic growth in ε. For example, putting $\nu = 0$ and $M_x = 0$ in Eq. (26) for the amplitude distribution of Eq. (18) gives

$$\beta_S^{[0,\mu]} = \frac{2\mu}{2\mu + 1}, \quad (M_x = 0, \quad \nu = 0, \quad ka \to \infty), \tag{30}$$

Physically important cases of Eq. (30) are axial dipoles, $\beta_S^{[0,1)} = 2/3$, and axial quadrupoles, $\beta_S^{(0,2)} = 4/5$.

6.1 – SOUND POWER VARIATION WITH MACH NUMBER

For sources that are not aerodynamic in origin, in the sense that their source strengths are not dependent upon the existence of a flow[1], the present approach may be used to obtain closed form expressions for the high-*ka* asymptotic sound power variation with M_x. These results are also useful, not only as a means of comparing the β_S - sensitivity of the various source distributions to flow, but also for allowing free-field sound power calculations involving aerodynamic sources to be corrected to include duct convection effects. Writing the high-*ka* behaviour of the mode amplitudes as continuous functions of α and M_x, This result follows from Eq. (3*b*) where the effect of a mean flow is to reduce the cutoff frequencies by the reciprocal of this factor. No general clos ed-form solution exists to Eq. (26) that is valid for all (ν, μ). However, solutions for the six main source distributions of interest here are given by

$$\frac{\overline{W}_x^{(\mu,\nu)}(M_x)}{\overline{W}_x^{(\mu,\nu)}(0)} = \begin{cases} 3M_x^{-3}\left(1-M_x^2\right)^{-1}\left[M_x^4 - M_x^3 - M_x^2 + 2M_x - 2\left(1-M_x^2\right)\ln(1+M_x)\right] & (\mu,\nu)=(1,0) \\ 1+M_x & (\mu,\nu)=(0,0) \\ \left(1-M_x^2\right)^{-1} & (\mu,\nu)=(0,1) \\ \left(1-M_x^2\right)^{-3}\left(1-M_x+\frac{1}{3}M_x^2\right) & (\mu,\nu)=(0,2) \\ \left(1-M_x^2\right)^{-1} & \text{equal energy per mode} \\ -3\left(\frac{1}{2}M_x^{-1}+M_x^{-2}+M_x^{-3}\ln(1-M_x)\right) & \text{equal energy denstiy per mode} \end{cases} \tag{31}$$

Equations (31) are plotted in Fig 6

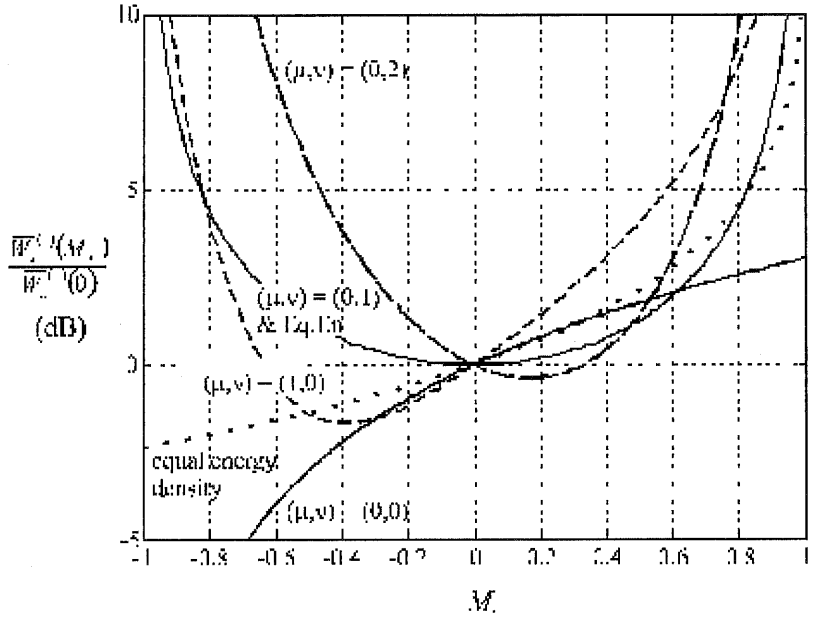

Figure 6. Multi-mode, high-*ka* Mach number dependence of the sound power flow for the source distributions of equal energy per mode, equal energy density per mode, an incoherent distribution of volume displacement sources, volume velocity sources, volume acceleration sources and axial dipole sources uniformly distributed over a duct cross section.

Generally, the power is predicted to increase with increasing Mach number in the duct exhaust, but decrease with increasing Mach number in the duct inlet. Exceptions are volume displacement sources that have a minimum value of -0.05dB at M_x = +0.2, and axial dipoles source whose minimum value is about –2dB at M_x = -0.39. Other interesting findings are that the equal energy per mode model and the volume acceleration source model are predicted to have identical high-*ka* Mach number dependence. Furthermore, this dependence is an even function of M_x suggesting that their sound power outputs are transmitted upstream and downstream equally.

REFERENCES

[1.1] D. H. Munroe and K. U. Ingard. 1979. Journal of acoustical society of America. 65 1402 - 1406. On acoustic intensiy measurements in the presence of mean flow.

[1.2] W. Neisse and F. Arnold. 2001. Journal of Sound and Vibration. 244(3), 481 – 503. On sound power determination in flow ducts.

[2.1] C.L. Morfey. 1971. Sound transmission and generation in ducts with flow. *J. Sound. Vib.* 14, 37 – 55.

[4.1]. P. Joseph and C. L. Morfey. 1999. Multi-mode radiation from an unflanged, semi-infinite circular duct. *J. Acoust. Soc. Am.* 105(5)

[4.2] W. Frommhold and F. P. Mechel 1989 *Fraunhofer-Institut fur Bauphysik BS* 202/89. Rechnerische Untersuchungen zur Bestimmung der Schalleistung in Rechteckkanaklen

---

[%] Non-axial components are equivalent to sources of lower order, in the modal formulation

[1] Fan noise is a common example of an aerodynamic source. The Mach number dependence of the transmitted sound power for these sources, particularly at low flow speeds, is dominated by its influence on the source strength. By comparison, the convection effects discussed here, which are a result of modifies modal propagation, are generally much weaker.